Two-photon deep tissue ex vivo imaging of mouse dermal and subcutaneous structures

Peter T. C. So and Hyun Kim

Department of Mechanical Engineering, Massachusetts Institute of Technology, Cambridge, MA 02139

ptso@mit.edu

Irene E. Kochevar

Wellman Laboratories of Photomedicine, Massachusetts General Hospital, Boston, MA 02114

kochevar@helix.mgh.harvard.edu

Abstract: The non-invasive determination of deep tissue three dimensional structure and biochemistry is the ultimate goal of optical biopsy. Two-photon microscopy has been shown to be a particularly promising approach. The use of infrared radiation in two-photon microscopy is critical for deep tissue imaging since tissue absorption and scattering coefficients for infrared light are much lower than for shorter wavelengths. Equally important, tissue photodamage is localized to the focal region where fluorescence excitation occurs. This report demonstrates that, by means of high resolution two-photon microscopy, skin and subcutaneous tissue structures can be imaged utilizing their endogenous fluorescence. From a freshly prepared tissue punch of a mouse ear, we were able to resolve in 3D both the living and cornified keratinocytes in the epidermis, the collagen/elastin fibers in the dermal layer and the cartilage in the subcutaneous layer. The ability to non-invasively acquire 3D structures of these tissue components may find application in areas such as non-invasive diagnosis of skin cancer and the study of wound healing processes.

OCIS codes: (170.2520) Fluorescence microscopy; (170.6900) Three-dimensional microscopy; (170.6930) Tissue; (170.1870) Dermatology; (170.7050) Turbid medium

References and links

1. G. Murphy and D. Elder, *Atlas of Tumor Pathology: Non-Melanocytic Tumors of the Skin,* (Armed Forces Institute of Pathology, Washington, D.C., 1990).
2. D. Elder and G. Murphy, *Atlas of Tumor Pathology: Melanocytic Tumors of the Skin,* (Armed Forces Institute of Pathology, Washington, D.C. 1990).
3. M. Okun, *Gross and Microscopic Pathology of the Skin,* (Dermatopathology Foundation Press, Boston, 1976).
4. S. Robbins and M. Angell, *Basic Pathology,* (W. B. Saunders Co., Philadelphia, PA 1971)
5. R. A. F. Clark and P. M. Henson, *The molecular and cellular biology of wound repair,* (Plenum Press,. New York, 1988).
6. W. Denk, W., J. H. Strickler and W. W. Webb, "Two-photon laser scanning fluorescence microscopy," Science **248**, 73-76 (1990).
7. D. W. Piston, B. R. Masters, and W. W. Webb, "Three-dimensionally resolved NAD(P)H cellular metabolic redox imaging of the *in situ* cornea with two-photon excitation laser scanning microscopy," J. Micros. **178**, 20-27, (1995).

#6200 - $15.00 US Received September 16, 1998; Revised October 26, 1998

8. B. R. Masters, P. T. C. So, and E. Gratton, "Multi-Photon Excitation Fluorescence Microscopy and Spectroscopy of *In Vivo* Human Skin," Biophys. J. **72**, 2405-2412 (1997).
9. M. Raijadhyaksha, M. Grossman, D. Esterowitz, R. H. Webb, and R. R. Anderson, "In vivo confocal scanning laser microscopy of human skin: melanin provides strong contrast," J. Investigative Dermatology **6**, 946-954 (1995).
10. P. Corcuff, C. Bertrand, and L. Leveque, "Morphometry of human epidermis in vivo by real-time confocal Microscopy," Arch. Dermatol. Res **285**, 475-481 (1993).
11. B. R. Masters, G., Gonnord, P. Corcuff, "Three-dimensional microscopic biopsy of in vivo human skin: a new technique based on a flexible confocal microscope," J. Micros. **185**, 329-338 (1997).
12. B. R. Masters, "Three-Dimensional Confocal Microscopy of Human Skin *In Vivo*: Autofluorescence of Normal Skin," Bioimages **4**, 13-19, (1996).
13. V. Rummelt, L. M. G. Gardner, R. Folberg, S. Beck, B. Knosp, T. O. Moninger, and K. C. Moore, "Three-dimensional relationship between tumor cells and micrcirculation with double cyanine immunolabelling, laser scanning confocal microscopy, and computer assisted reconstruction: an alternative to cast corrosion preparation," J. Histochemistry and cytochemistry **42**, 681-686 (1994).
14. T. Wilson and C. Sheppard, *Theory and practice of scanning optical microscopy*, (Academic Press, New York, NY, 1984).
15. J. B. Pawley, *Handbook of Biological Confocal Microscopy*,.(Plenum Press, New York, 1995).
16. B. R. Masters, "*In vivo* corneal redox fluorometry", *in Noninvasive Diagnostic Techniques in Ophthalmology*, B. R. Masters, ed. (Springer-Verlag, New York, 1990).
17. M. G**ö**ppert-Mayer, "**Ü**ber Elementarake mit zwei Quantensprungen," Ann. Phys. (Leipzig) **5**, 273-294 (1931).
18. M. J. Booth, S. W. Hell, "Continuous wave excitation two-photon fluorescence microscopy exemplified with the 647-nm ArKr laser line," J. Microsc. **190**, 298-304 (1998)
19. B. Chance, and B. Thorell, "Localization and kinetics of reduced pyridine nucleotide in living cells by Microfluorometry," J. Biol. Chem. **234**, 3044-3050 (1959).
20. B. Chance, "Pyridine nucleotide as an indicator of the oxygen requirements for energy-linked functions of Mitochondria," Circ. Res. Suppl. 1 **38**, I-31 - I-38 (1976).
21. B. Chance, B. Schoener, R. Oshino, F. Itshak, & Y. Nakase, "Oxidation-Reduction Ratio Studies of Mitochondria in Freeze-trapped Samples," J. Biol. Chem. **254**, 4764-4711 (1979).
22. B. D. Bennett, T. L. Jetton, G. Ying, M. A. Magnuson and D. W. Piston, "Quantitative Subcellular Imaging of Glucose Metabolism within Intact Pancreatic Islets," J. Biol. Chem. **271**, 3647-3651 (1996).
23. B. R. Masters and B. Chance, "Redox confocal imaging: intrinsic fluorescent probes of cellular metabolism" in *Fluorescent and Luminescent Probes for Biological Activity*, W.T. Mason, ed., (Academic Press, London, 1993).
24. S. Maiti, J. B. Shear, R. M. Williams RM, W. R. Zipfel, W. W. Webb, "Measuring serotonin distribution in live cells with three-photon excitation," Science **275**, 530-532 (1997).
25. W. Zipfel, "Multi-photon excitation of intrinsic fluorescence in cells and intact tissue", Presented in Application of multi-photon excitation imaging, Pre-Microscope Society of America Symposium, Cleveland, OH, Aug 9-10, 1997.
26. F. S. LaBella, and P. Gerald, "Structure of collagen from human tendon as influence by age and sex," J. Gerontol. **20**, 54-59 (1965).
27. M. K. Dabbous, "Inter- and intramolecula cross-linking in tyrosinase-treated tropocollagen," J. Bio. Chem. **241**, 5307-5312 (1966).
28. K. C. Hoerman and A. Y. Balekjian, "Some quantum aspects of collagen," Federation Proc. **25**, 1016-1021 (1966).
29. J. Thomas, D. F. Elsden, S. M. Partridge, "Degradation products from elastin," Nature **200**, 651-652 (1963).
30. F. S. LeBella, "Studies on the soluble products released from purified elastic fibers by pancreatic elastase," Arch. Biochm. Biophys. **93**, 72-79 (1961).
31. F. S. LaBella, and W. G. Lindsay, "The structure of human aortic elastin as influence by age," J. Gerontol. **18**, 111-118, 1963.
32. P. T. C. So, T. French, W. M. Yu, K. M. Berland, C. Y. Dong, and E. Gratton, "Time-resolved fluorescence microscopy using two-photon excitation," Bioimaging **3**, 49-63 (1995).

1. Introduction

Two-photon tissue imaging is a promising technology for a number of biomedical applications including the development of non-invasive biopsy techniques and the design of tissue regenerative devices. For optical biopsy, tissue pathological analysis relies on morphological information with sub-cellular details [1-4]. This sub-cellular structural information has been traditionally acquired from histological sections of excised tissue.

#6200 - $15.00 US Received September 16, 1998; Revised October 26, 1998

Much of the cellular biochemical information is inevitably lost during the surgical and fixation processes. More importantly, the biopsy procedure is generally undesirable due to its invasive nature. For tissue regenerative device design, recent developments in molecular biology have focused this field on the identification of molecular signals that control tissue regeneration. Various adhesion molecules as well as growth factors appear to play key roles [5]. While the molecular approach is a powerful paradigm, the understanding of tissue regeneration processes is not complete without establishing a connection between biochemical signals and the corresponding morphological changes in cells and extracellular matrix structures. This goal has not been achieved. Tissue opacity prevents effective in vivo fluorescence microscopy imaging in "deep" specimens that has thickness on the order of the reduced scattering length of light. The reduced scattering length of light is on the order of several hundred microns for typical tissues such as human skin. The recent invention of two-photon microscopy has opened new opportunities in tissue imaging [6-8]. Using two-photon microscopy and spectroscopy, an attempt can be made to address this missing connection in our understanding between tissue morphological states and the underlying biochemical driving forces.

1.1 Confocal deep tissue optical imaging

Confocal microscopy has been traditionally the most promising technology for the study of 3-D deep tissue structure with sub-cellular resolution [9-13]. The basic concept behind confocal microscopy is relatively simple [14,15]. In a confocal system, excitation light deflected by a beam splitter is focused through the objective onto the sample. In the reflected light mode, scattered light is generated throughout the hour-glass-shaped excitation volume. In the fluorescence mode, fluorescence excitation also occurs throughout the same large volume. In order to isolate a single optical section, the light collected by the objective is re-focused on to a pinhole aperture placed at a telecentric plane. At this plane, only the photons originating from the objective focal volume will be focused through the aperture whereas the off-focus photons are rejected. High resolution 3-D image stacks from human skin and eyes have been obtained *in vivo* [7-12,16]. This technique provides spatial resolution with radial and depth resolution on the order of 0.2 μm and 0.5 μm respectively. Operating in reflected light mode, the penetration depth of a confocal microscope is about 200 μm. Operating in fluorescence mode, the penetration distance is much shorter. With near UV excitation, the penetration depth in human skin is reduced to only 30 μm.

1.2 Two-photon excitation microscopy

In the past decade, two-photon microscopy, introduced by Denk *et al.*, emerges as a promising alternative. Chromophores can be excited by the simultaneous absorption of two photons each having half the energy needed for the excitation transition [6,17]. Since the two-photon excitation probability is significantly less than the one-photon probability, appreciable two-photon excitation occurs only at the focal point, a region of high temporal and spatial concentration of photons. The high spatial concentration of photons can be achieved by focusing the laser light with a high numerical aperture objective to a diffraction limited spot. The high temporal concentration of photons is made possible by the availability of high peak power mode-locked lasers. While two-photon excitation can be achieved using CW laser excitation, tissue thermal damage is a serious concern because of the high average power needed [18]. For a mode-locked laser source with an average power p_o, repetition rate f_p, pulse width τ_p, and wavelength λ, focused by an objective with numerical aperture A, the

#6200 - $15.00 US Received September 16, 1998; Revised October 26, 1998

number of photon pairs absorbed per laser pulse and per chromophore, n_a, can be estimated as [6]:

$$n_a \approx \frac{p_0^2 \delta}{\tau_p f_p^2} \left(\frac{\pi A^2}{hc\lambda} \right)^2$$

where c is the speed of light, h is Planck's constant and δ is the two-photon cross section, typically on the order of 10^{-50} to 10^{-49} cm^4 sec $photon^{-1}$ $molecule^{-1}$.

Depth discrimination is the most important feature of the two-photon microscopy. 3-D imaging capability will allow biological samples to be imaged *in vivo*. For one-photon excitation in a spatially uniform fluorescent sample, assuming negligible excitation attenuation, equal fluorescence intensities are contributed from each z-section above and below the focal plane because one-photon absorption is proportional to the average power. On the other hand, in the two-photon case over 80% of the total fluorescence intensity comes from a 1 μm thick region about the focal point for a 1.25 numerical aperture objective. Thus, 3-D images can be constructed as in confocal microscopy, but without confocal pinholes. This depth discrimination effect of two-photon excitation arises from the quadratic dependence of two-photon fluorescence intensity upon the excitation photon flux which decreases rapidly away from the focal plane.

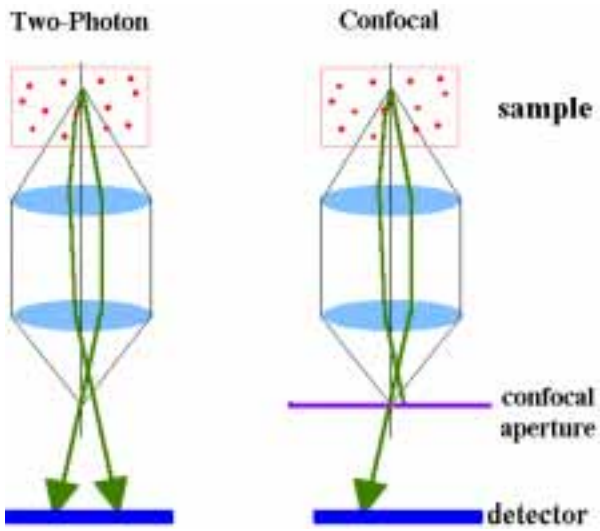

Fig. 1. A comparison between two-photon and confocal microscope detection geometry. In a highly scattering medium, a large fraction of emitted photons will be scattered before they are collected by the objective. In the two-photon system, most of these scattered photons can be collected by a large area detector. In the confocal system, these scattered photons are blocked at the confocal pinhole aperture and cannot be detected.

Two-photon excitation allows 3-D biological structures to be imaged with resolution comparable to confocal microscopes but with a number of significant advantages for thick tissue imaging with large absorption and scattering coefficients: (1) The typical absorbency in the infrared spectral range is more than an order of magnitude less than that of the near UV or the blue-green region. Using infrared excitation in a two-photon microscope minimizes the attenuation of the excitation signal. (2) There is also less loss of infrared

#6200 - $15.00 US
Received September 16, 1998; Revised October 26, 1998

radiation due to scattering. In the simplest Raleigh scattering approximation, the scattering cross section decreases as the fourth power of the increasing wavelength. (3) Confocal microscopy uses the emission pinhole aperture to reject out of focus light. Inside deep tissue, scattering of signal photons is inevitable. The consequent path deviation results in a significant loss of these photons at the confocal pinhole. The collection geometry for the fluorescence photons is less critical in the two-photon case where a large area detector can be used without a pinhole aperture. Most of the forward scattered photons can be retained (Figure 1). (4) Two-photon excitation minimizes tissue photo-damage. Conventional confocal techniques obtain 3-D resolution by limiting the observation volume, but fluorescence excitation occurs throughout the hourglass shape light path. In contrast, two-photon excitation limits the region of photo-interaction to a sub-femtoliter volume at the focal point. (5) Two-photon excitation wavelengths are typically about twice the one-photon excitation wavelengths. This wide separation between excitation and emission spectra ensures that the excitation light and the Raman scattering can be rejected while filtering out a minimum of fluorescence photons.

1.3. Tissue imaging based on tissue endogenous fluorescence

The importance of endogenous fluorescence imaging has been recognized because of its use for non-invasive monitoring of tissue cellular metabolism by means of redox fluorometry [16, 19-23]. The probes are endogenous fluorescent pyridine nucleotides, and flavoproteins. The pyridine nucleotides, NAD(P)H are excited in the 365 nm region and fluoresce in the 400-500 nm region. The flavoproteins are excited around 450 nm and fluoresce between 500-600 nm. Typically, the changes in fluorescence intensity follow changes in cell and tissue oxidative metabolism. Fluorescence imaging of cellular redox metabolism has been successfully performed in the cornea and in the skin.

Recent studies of Webb's group in Cornell have demonstrated that two-photon microscopy is capable of imaging other tissue components such as collagen/elastin using their endogenous fluorescence [24,25]. However, non-invasive imaging of these structures in intact tissue has not been demonstrated. In contrast to cellular systems, the fluorescence properties of extracellular matrix components have received relatively little attention. Nevertheless, some basic spectroscopic characterizations of these tissue components have been performed. Tropocollagen and collagen fibers, typically have absorption in the range of 280 to 300 nm and emission ranges from 350 to 400 nm [26-28]. Elastin has been observed to have a redder emission spectrum at 400 to 450 nm with excitation wavelengths of 340 to 370 nm [29-31].

2. Materials and Methods

2.1 Two-Photon Deep Tissue Microscopy

In relatively transparent tissues such as the cornea, two-photon deep tissue imaging has been achieved [7]. However, for opaque tissue such as the human skin, two-photon deep tissue imaging remains a challenge. A two-photon microscope has been designed to study deep tissue [32]. A schematic of the modified microscope is presented in Fig. 2.

The laser used in this microscope is a mode-locked Titanium-Sapphire laser (Mira 900, Coherent Inc., Palo Alto, CA). The features are its high average power (1.5 W), its high repetition rate (80 MHz), and its short pulse width (150 fs). The high peak power optimizes two-photon excitation while minimizing scattered light contamination from the

#6200 - $15.00 US Received September 16, 1998; Revised October 26, 1998

excitation source. This is particularly important in deep tissue study where excitation efficiency should be maximized but the power deposited in the tissue should be minimized. Furthermore, the intensity output of this laser is very stable with typical fluctuations less than 0.5% ensuring intensity uniformity over the image. The typical laser excitation wavelengths used in this work is 780 nm.

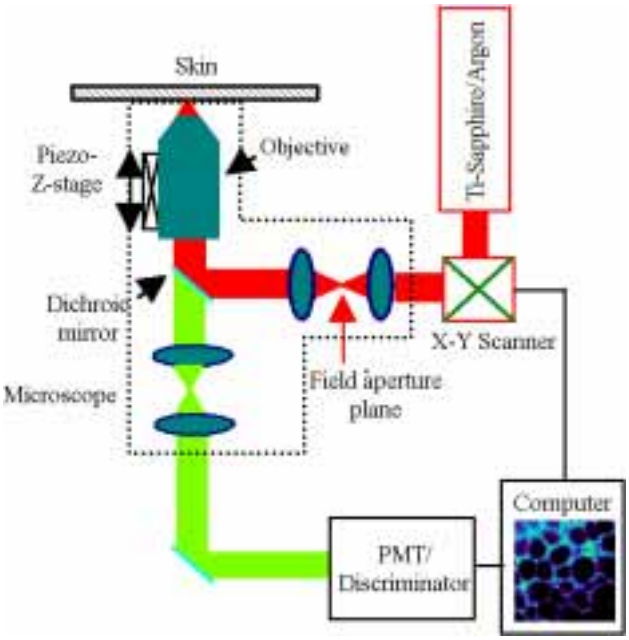

Fig. 2. Schematic of the prototype two-photon deep tissue microscope

The beam expanded laser light is directed into the microscope via a galvanometer-driven x-y scanner (Cambridge Technology, Watertown, MA). Images are generated by raster scanning the x-y mirrors. The excitation light enters the Zeiss Axiovert 135 microscope (Zeiss Inc., Thronwood, NY) via a modified epi-luminescence light path. The scan lens is positioned such that the x-y scanner is at its eye-point while the field aperture plane is at its focal point. Since the objectives are infinity-corrected, a tube lens is positioned to re-collimate the excitation light. The scan lens and the tube lens function together as a beam expander which over-fills the back aperture of the objective lens. Proper over-filling of the back aperture is required for the objective to achieve the manufacturer specified numerical aperture. The excitation light is reflected by the dichroic mirror to the objective. The dichroic mirrors are custom made short pass filters (Chroma Technology Inc., Brattleboro, VT) which maximize reflection in the infrared and transmission in the blue-green region of the spectrum. The objective used in most of these studies is a Zeiss Fluar 40X with numerical aperture of 1.3. This objective is chosen for its high numerical aperture and its high throughput. The high numerical aperture is essential for the formation of a diffraction limited point spread function. In the tissue, it is expected that the image point spread function should degrade with increasing tissue turbidity and depth. Additional experiments are still needed to verify and characterize this conjecture. This objective is designed to have a minimal number of lens components to maximize its throughput (80% at 500 nm). The objective axial position is driven by a computer interfaced piezo positioner (PI

#6200 - $15.00 US Received September 16, 1998; Revised October 26, 1998

Inc., Auburn, MA). The axial resolution of this system is about 0.05 μm with a range of 100 μm.

The fluorescence emission is collected by the same objective and transmitted through the dichroic mirror along the emission path. An additional barrier filter is needed to further attenuate the scattered excitation light because of the high excitation intensity used. Since two-photon excitation has the advantage that the excitation and emission wavelengths are often well separated (typically by 300 – 400 nm), suitable short pass filters such as 2 mm of BG39 Schott glass filter (CVI Laser, Livermore, CA) eliminate most of the residual scatter with a minimum attenuation of the fluorescence. A de-scan lens is inserted between the tube lens and the photomultiplier tube (PMT). The de-scan lens re-collimates the excitation. It also ensures that the emission light strikes the PMT at the same position independent of scanner motion.

The number of available fluorescence photons is always a limiting factor in non-invasive deep tissue imaging. On one hand, the scattering and absorption properties of thick tissue quickly diminishes both the excitation and the emission light. On the other hand, we always seek to use the lowest excitation power possible to limit any possible photodamage to the tissue. In this low light situation, we have implemented a single photon counting detection system. The fluorescence signal at each pixel is detected by a R5600-P PMT (Hamamatsu, Bridgewater, NJ) which is a compact single photon counting module with high quantum efficiency of 12% at 500 nm and 25% at 400 nm. The dark noise of this PMT is less than twenty photon counts per second at room temperature. This high signal to noise ratio is crucial for high sensitivity detection. A 100 MHz single photon counting discriminator (F-100T, Advanced Research Instruments, Boulder, CO) converts single photon bursts into TTL pulses. The number of collected photons are counted using a home built interface circuit and the number is transferred to the data acquisition computer. The image stack were visualized in 3-D and animated using Slicer (Fortner Research, Sterling, VA).

2.2 Tissue Structure and fluorescence properties of the punch biopsy

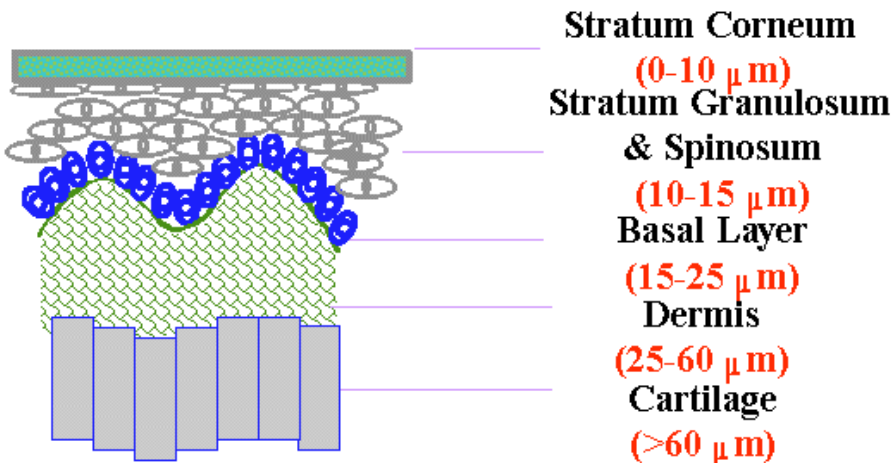

Fig. 3: Corss section of mouse ear (one-half of full thickness). The presence of a cartilage layer below the skin is unique to the ear.

A 3 mm punch biopsy was obtained from the ear of a mouse having a thickness less than 1 mm. For this experiment, we primarily focused on resolving the dermal structure and

#6200 - $15.00 US Received September 16, 1998; Revised October 26, 1998

the adjacent subcutaneous layer. Skin is comprised of two layers: the epidermis and the dermis. The epidermis is the outermost portion of the skin and is a stratified squamous epithelium composed mainly of keratinocytes. In human, the epidermal thickness varies from 50 μm on the eyelids to 1.5 mm on the palms and soles. In mouse skin, the epidermis is typically 30 μm thick. The innermost layer of the epidermis consists of a single layer of cuboidal cells called basal cells. These cells differentiate and migrate towards the skin surface where they eventually die and flatten to form the outer layer of the epidermis, the stratum corneum. The lower layer of skin, the dermis, has a low cell density and is largely composed of the extracellular matrix molecules collagen, elastin and proteoglycans. Fibroblasts are the primary cell type in the dermis. The fibroblasts in the dermis tends to be very elongated. Below the skin layers, cartilage forms the structural support for the mouse ear; this structure is not present under other types of skin. Figure 3 shows a drawing of the vertical section of mouse ear illustrating the different cellular layers.

3. Results and Discussion

3.1 Two-Photon Microscopy Imaging

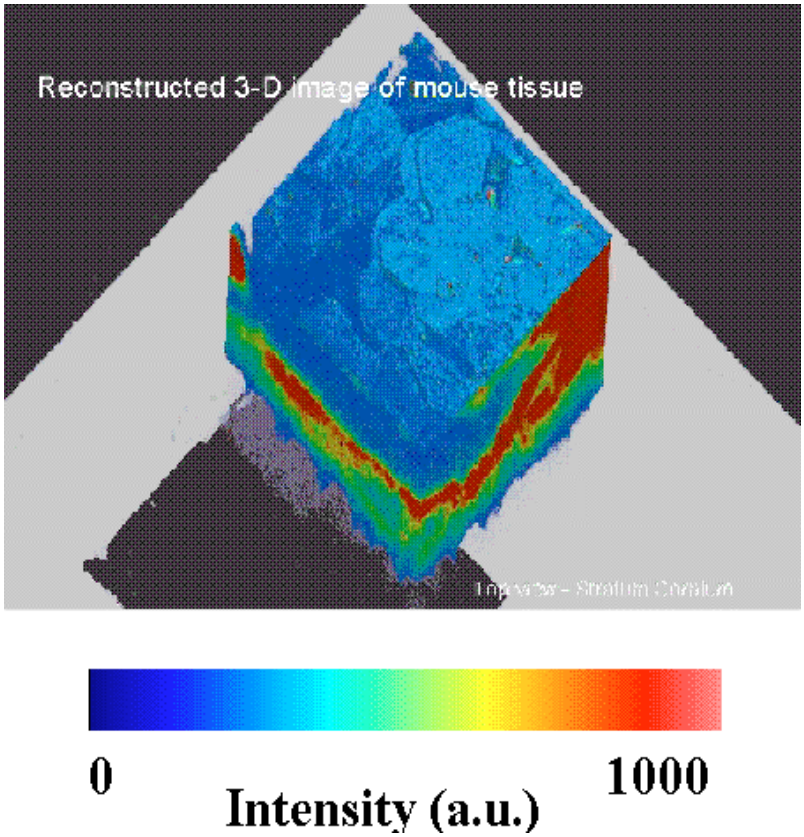

Fig. 4. A 3-D reconstructed movie sequence showing the relevant dermal and subcutaneous structures of the mouse tissue punch as imaged by two-photon microscopy.

High resolution images of three dimensional structures in the mouse ear tissue punch were obtained using 15 mW laser excitation at 780 nm. Pixel residence time for this images is 64 μs. The typical images stacks have a lateral dimension of 120 μm and an axial

#6200 - $15.00 US Received September 16, 1998; Revised October 26, 1998

dimension of 100 μm. The axial separation between image planes was 0.25 μm. The fluorescent structural details in the dermal and sub-dermal layers are best visualized in an animated three dimensional reconstruction (Fig. 4). In this reconstruction, the color scale represents the intensity only and contains no spectral information. Five distinct layers of the tissue can be readily resolved. At the tissue surface, i.e. the stratum corneum, large, hexagonal shaped cells were observed (Fig. 5a). These cells were highly fluorescent. The cells in the stratum corneum have typically lost their nuclei which is consistent with our observation. Cells in the process of sloughing were also observed. Two layers of living cells were observed between the stratum corneum and the basal layer (Fig. 5b). Quantitatively, the fluorescence intensity originates from these layers were one-half to one-third that of the stratum corneum. The cells in these layers were fairly large (about 15 μm across) and were well organized. The fluorescence of these cells mainly originates from the cytoplasm. From the previous studies [8], the major chromophore in the cytoplasm responsible for the observed fluorescence is NAD(P)H. The cellular nuclei with a negligible NAD(P)H concentration were clearly observed as large oblong dark regions. The basal layer lies above the epidermal-dermal junction (Fig 5c). Cellular autofluorescence from the basal layer is slightly more intense as compared with the upper cell layers but is within a factor of 2. Cell packing in this layer was less well organized. These cells were smaller in cross sections but were thicker as compared with cells in the upper epidermal layers. In a previous human study, no clear structure was observed below the epidermal-dermal junction. In this study, we have succeeded in performing high resolution imaging of tissue structure. We have observed fiber-like structures throughout the dermal layer (Fig. 5d). This structures are likely to be collagen or elastin fibers. Further, the fluorescence intensities of these fibers are very high. It is about an order of magnitude brighter than that of the epidermal cell layers. Even though they are at a greater depth, these fibers are the most fluorescent structures observed in this study except the stratum corneum. Below the dermis, we observed honeycomb-like structures with a loose hexagonal packing arrangement (Fig. 5e). Fluorescence originates from the walls of these honeycomb structure. The morphology of this layer is consistent with the cartilage structure below the dermis which is the primary structural support of the mouse ear. The fluorescence intensity from the cartilage is comparable to that of the epidermal cell layers.

#6200 - $15.00 US Received September 16, 1998; Revised October 26, 1998

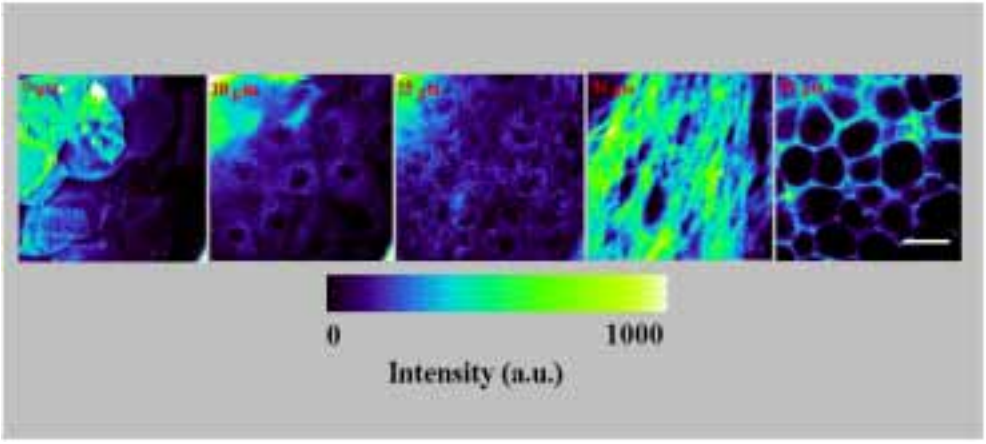

Fig. 5: A montage of x-y sections of mouse ear structures obtained by two-photon deep tissue microscopy. From left to right, the five panels are images of: stratum corneum, epidermal cell layer, basal cell layer, dermal structure, and cartilage. The depth where these images were taken are indicated in the upper left corner of the panel. The scale bar is 20 μm.

3.2 Histological comparison

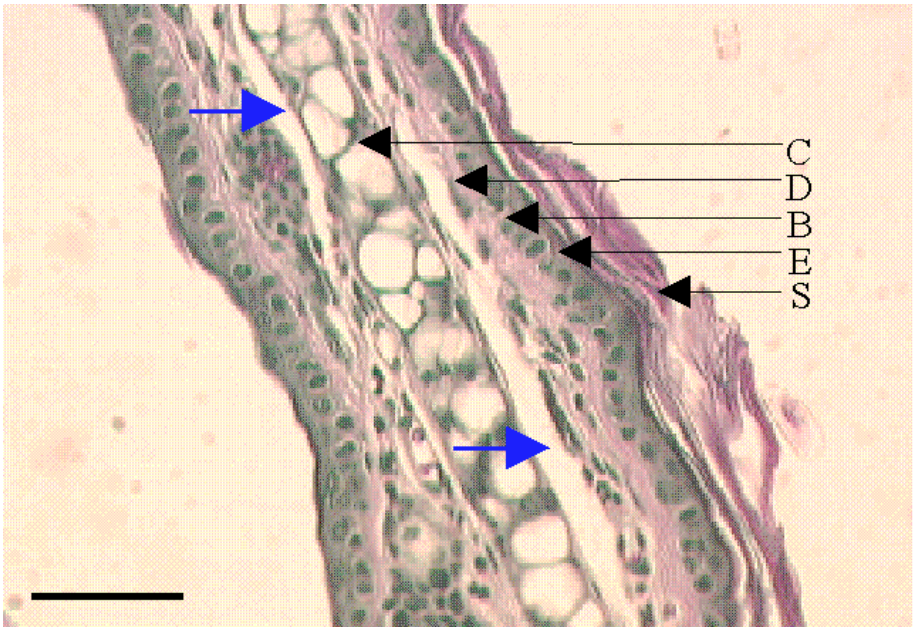

Fig. 6: Light microscopy image of a histological section of the mouse ear tissue punch. The scale bar at the lower left corner represents 50 μm. S is the stratum corneum, E is the epidermal cell layers. B is the basal cell layer, D is the dermal layer, and C is the cartilage. The blue arrows indicate tissue tears common in the preparation of histological section.

Histological data were obtained as an independent verification of the two-photon imaging results. Histological sections were prepared from the same mouse ear where the

#6200 - $15.00 US
Received September 16, 1998; Revised October 26, 1998

tissue punch was taken. The sections were stained and viewed under a light microscope (Leitz, , 50x objective). A typical image is presented in figure 6. Note the almost perfect correspondence between the structures observed in the histological section and those obtained using two-photon microscope. Similar to the two-photon case, structures corresponding to the stratum corneum, the epidermal cell layer, the basal cell layer were clearly observed. In the histological section, the alignment and packing of collagen/elastin fibers in the dermal layers are difficult to see as opposed to the two-photon image where these fibers can be clearly resolved. Some fibroblasts were seen in the dermal layer in the histological slices. However, no cell structures were seen in the dermis by two-photon. This can be accounted for by two factors. It is possible that the cell were difficult to locate because of their sparse distribution. It is more likely that the much higher relative fluorescence intensity of the collagen/elastin fibers obscure the much dimmer fluorescence from the fibroblasts. The honeycomb shaped cartilage layer could clearly be seen in both the histological and two-photon images. Finally, there are a number of large tears and other distortions in the thin histology section. This is a common occurrences in the preparation of histological specimen. The use of two-photon imaging circumvents this problem and provides an image relatively free of sample preparation artifacts.

Further, the tissue structures observed by two-photon microscopy above the epidermal-dermal junction are consistent with the results from a previous in vivo study of human skin [8]. The main difference between human and mouse epidermis is the greater thickness of the stratum corneum and the epidermal cell layers in the human. Note that the image quality is significantly improved in the present study as compared with the in vivo human study. This improvement is caused by two factors. First, since this is an excised tissue there are no motion artifact which is always present in living human subjects. Second, the depth increment of the human study was at 5 μm while the depth increment used in this study is 0.25 μm which provides much better resolution. This experimental protocol difference is dictated by the difficulty of requiring a human subject to hold steady over a long period of time.

4. Conclusion

We have succeeded in obtaining high resolution, 3D images from the skin and the subcutaneous layers of a mouse ear. Five unique structural layers were observed: the stratum corneum, the epidermal cell layers, the basal cell layer, the dermal layer and the underlying cartilage. The collagen/elastin fiber structures have not been previously observed in tissues samples with intact epidermis and stratum corneum layers. The epidermal structures obtained are in close agreement with previous experiments on human subjects. The structure resolved from the whole tissue is in good agreement with histology.

While this study has demonstrated the potential of two-photon imaging for tissue diagnosis, it also clearly shows what technological advances are needed. First, while the chromophore in the cellular cytoplasm has been identified to be NAD(P)H, the chromophores responsible for the fluorescence in the dermis and the subcutaneous layer remain poorly characterized. We do not know whether the fiber structures observed corresponds to collagen or elastin. These remaining questions indicate that the incorporation of spectral resolved measurements in two-photon deep tissue imaging is a priority. Second, the time required to obtain the 3-D image stack is on the order of a half hour. This lengthy imaging time makes application involving living human subjects difficult both in terms of motion artifacts as well as the long term immobilization. This difficulty indicates a need for video rate two-photon deep tissue imaging.

#6200 - $15.00 US Received September 16, 1998; Revised October 26, 1998

5. Acknowledgement

This work was supported by grants from ACS RPG9805801CCE (PTCS), NIH R29GM56486-01 (PTCS), and NIH R01AR43895 (IEK).

#6200 - $15.00 US Received September 16, 1998; Revised October 26, 1998